

# Water Absorption Properties of Phosphate Glass Fiber-Reinforced Poly- $\epsilon$ -caprolactone Composites for Craniofacial Bone Repair

Levent Onal,<sup>1</sup> Sophie Cozien-Cazuc,<sup>2</sup> I. Arthur Jones,<sup>2</sup> Christopher D. Rudd<sup>2</sup>

<sup>1</sup>Department of Textile Engineering, Erciyes University, 38039 Kayseri, Turkey

<sup>2</sup>School of Mechanical, Materials and Manufacturing Engineering, University of Nottingham, Nottingham NG7 2RD, United Kingdom

Received 26 March 2007; accepted 29 August 2007

DOI 10.1002/app.27518

Published online 6 December 2007 in Wiley InterScience (www.interscience.wiley.com).

**ABSTRACT:** The moisture uptake of polymers and composites has increasing significance where these materials are specified for invasive, long-term medical applications. Here we analyze mass gain and the ensuing degradation mechanisms in phosphate glass fiber reinforced poly- $\epsilon$ -caprolactone laminates. Specimens were manufactured using *in situ* polymerization of  $\epsilon$ -caprolactone around a bed of phosphate glass fibers. The latter were sized with 3-aminopropyltriethoxysilane to control the rate of modulus degradation. Fiber content was the main variable in the study,

and it was found that the moisture diffusion coefficient increased significantly with increasing fiber volume fraction. Diffusion, plasticization, and leaching of constituents appear to be the dominant aspects of the process over these short-term tests. © 2007 Wiley Periodicals, Inc. *J Appl Polym Sci* 107: 3750–3755, 2008

**Key words:** biodegradable composites; phosphate glass fiber; moisture absorption; degradation; diffusion coefficient

## INTRODUCTION

Implants are used to replace or repair damaged or dysfunctional tissues or limbs in the body and can be made from metals or polymeric materials. However, well-known problems with metallic implants include stress-shielding<sup>1</sup> and occasional allergic response.<sup>2</sup> In addition, electrolytic potentials between metals and body fluids can cause corrosion of the implant and tissue necrosis.<sup>3</sup> Stress-shielding means that metal implants carry most of the loading even after the healing of fractures. The adaptive nature of bone leads to the formation of defective tissue underneath the implant. In order to prevent further complications, secondary surgery is performed to remove the metal implant. Thus, resorbable materials have attracted substantial attention because of their capabilities in various applications such as sutures, wound dressings, bone plates, implants, and joints.<sup>4–6</sup> Biological resorption without harmful effects and the possibility of implant removal without surgery are two very significant potential advantages of polymer-based resorbable implants over metals in this context.

The introduction of resorbable polymers and composites for medical implants involves two significant challenges: controlling the resorption degradation period and maintaining a sufficiently high modulus. Small craniofacial implants, for example, might require the structural properties to be maintained for between 6 and 52 weeks. Rinehart et al.<sup>7</sup> studied dissolution of phosphate glass fibers, which have potential as resorbable reinforcements. They processed fibers with and without silane sizing agent in a phosphate-buffered saline environment. Kweon et al.<sup>8</sup> generated novel degradable poly- $\epsilon$ -caprolactone (PCL) networks. They analyzed mass loss of various PCL networks and commercial polymers over a 6-week period. PCL is known to persist *in vivo* for at least 2 years.<sup>9</sup> Prabhakar et al.<sup>10</sup> have also studied the effect of CaO loading in phosphate glasses on the degradation properties of particulate-reinforced PCL composites.

The present study forms part of a broader examination of low-temperature formable composites that might serve as bone scaffolds in craniofacial surgery. Initial target application areas include low load-carrying areas such as cranial plugs and bone onlays. Here, textile-reinforced resorbable specimens were manufactured using PCL matrix and phosphate glass fibers. Earlier studies by Corden et al. assessed studied physical properties and biocompatibility,<sup>11</sup> while the degradation and short-term biocompatibility issues around the phosphate glass fibers were analyzed by Gough et al.<sup>12</sup>

Correspondence to: L. Onal (lonal@erciyes.edu.tr).

Contract grant sponsor: "TUBITAK-The Royal Society Scientific Research Program Award".

Contract grant sponsor: University of Nottingham.

*Journal of Applied Polymer Science*, Vol. 107, 3750–3755 (2008)  
© 2007 Wiley Periodicals, Inc.

In this paper, water absorption properties of resorbable, continuous phosphate glass fiber-reinforced PCL composites having various volume fraction ratios of fibers were studied. *In situ* polymerized<sup>13</sup> composite specimens were immersed in distilled water at 37°C and water absorption was monitored for 6 weeks. Moisture uptake (neglecting hydrolytic degradation) was used to calculate effective diffusion coefficients using Fick's second law.

## EXPERIMENTAL

### Materials

Sodium phosphate, calcium phosphate, and magnesium phosphate salts (Sigma Aldrich) were used to manufacture phosphate glass fibers (P<sub>40</sub>Na<sub>20</sub>Ca<sub>16</sub>Mg<sub>24</sub>), whose weight fraction ratio is 43, 37, and 20%, respectively. After mixing and drying, the salts were melted to produce glass cullet for fiber spinning. Fibers were spun in a continuous operation in a laboratory scale assembly. The average filament diameter was 18  $\mu$ m. Fibers are homogenous and nonporous. Fiber bundles are sized in a batch process with 3-aminopropyl triethoxy silane (Sigma-Aldrich) to control interface properties and the ensuing hydrolytic degradation process. Aminopropyl triethoxy silane solution (1% v/v) was mixed in aqueous ethanol solution. Glass fibers were immersed in that solution for 15 min. The fibers were then dried in an oven for 24 h at 120°C.

### Specimen fabrication

$\epsilon$ -Caprolactone (Acros Organics), calcium hydride powder (Sigma-Aldrich), and catalysts (BF<sub>3</sub> and Sn(Oct)<sub>3</sub>) were used in the *in situ* polymerization method described earlier.<sup>14</sup>

The specimens were fabricated at fiber volume ratios of 0–20% and slit into 25  $\times$  10  $\times$  1 mm<sup>3</sup> coupons. All test specimens were conditioned in a desiccator for 24 h to remove residual moisture before testing.

### Moisture regain set-up

Moisture regain and degradation studies used an incubator at 37°C and distilled water. The initial dry mass was first measured before immersing 10 samples from each group in individual containers. The solution was changed every 24 h. Specimens were withdrawn, blot-dried, weighed to a resolution of 0.0001 g and returned to solution.

A slightly different experimental set-up, modified from that of Rinehart et al.,<sup>7</sup> was used to characterize the PG fibers. Approximately, 89-mg yarn was held in an aluminium frame and suspended via an

aluminium wire from the underhook of a CP 225D Sartorius analytical balance. The assembly was immersed in a beaker filled with 400 mL of distilled water. The distilled water was degassed under vacuum for at least 1 h to avoid air bubble formation on the frame after immersion. Twenty milliliters of oil was added to the water after immersing the fibers to control the evaporative losses. The beaker was held in a water bath at 37°C. The weight loss of the fibers was monitored continuously by coupling the balance to a laptop computer.

### SEM analysis

Samples were gold-coated and viewed by Jeol SEM at an accelerating voltage of 15 kV (for PG fibers) and 20 kV (for composites), to observe the morphology of samples prior to and after the degradation study.

### Statistical analysis

The statistical software package JMP<sup>®</sup> was employed to interpret the experimental data at the 95% confidence level. The results were evaluated based on *F* ratio and probability of *F* ratio (prob > *F*). The lower the probability of *F* ratio the more significant the variable is.

## RESULTS AND DISCUSSION

### Moisture regain of composite

The moisture regain (*R*) of composite and fiber was calculated as a function of time (*t*) with the basic relation given as follows:

$$R = \frac{m_t - m_0}{m_0} \times 100 \quad (1)$$

where *m<sub>t</sub>* is the weight of moist material at a pre-determined time *t* and *m<sub>0</sub>* is the initial dry weight of sample.

In Figure 1, the moisture regain of composites is plotted against immersion period for different volume fractions of phosphate glass fibers. The increase of initial mass caused by immersion of water to composite is followed by mass loss. Moisture gain increased with the increase in the fiber volume fraction, and this was confirmed as statistically significant at the 95% confidence interval using one-way analysis of variance, where the probability of *F* ratio (prob > *F*) was 0.0127.

After aging for 162 h, the mass gain slowed for each of the fiber-reinforced coupons. Five hundred four hours appeared to represent an inflection point where the net effect of moisture uptake and ion

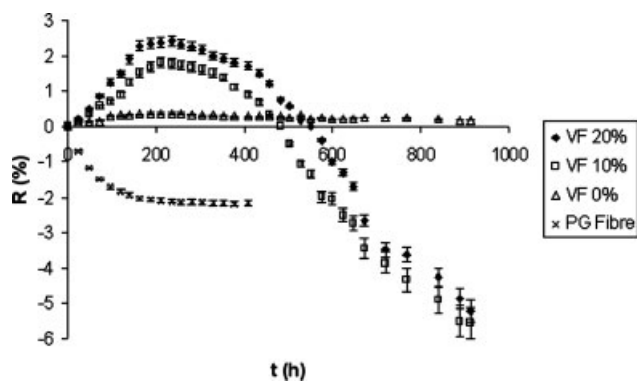


**Figure 1** Moisture regain of phosphate glass fiber PCL composite for various fiber volume ratios as a function of time.

leaching from the fibers became negative. Note that the unreinforced control specimen remained sensibly constant for the duration of the 900-h trial. When time to reach saturation and the maximum moisture recorded for pure PCL sample in this study is compared with that given by Aitchison et al.,<sup>15</sup> the moisture content is smaller (0.38% in this study) while time to reach maximum moisture content is longer (Table I). This can be attributed to the specimen size, which is 2.4 times thicker than the one used in this study.

### Degradation

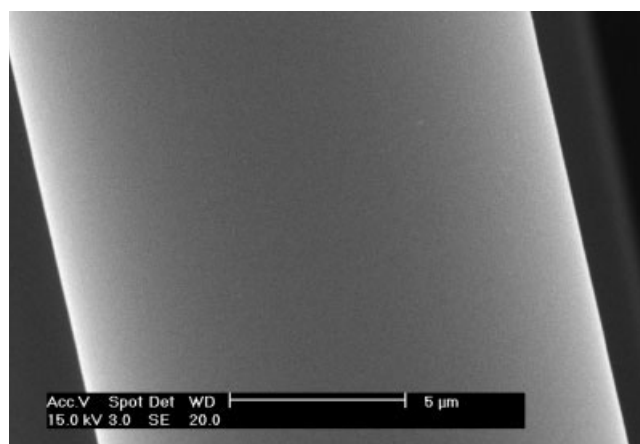
Clearly, diffusion of water shapes the initial mass gain process. Since the curves indicate that moisture uptake by the pure PCL composite is negligible in contrast with the fiber-reinforced specimens, this suggests that either the fibers are hydroscopic and/or that internal voids (including those at the fiber-matrix interface) act as reservoirs.

Figure 2 shows the surface of the PG fibers before and after aging in water. The micrographs show clear evidence of surface degradation in the absence of a sheath of polymer matrix. This is confirmed by

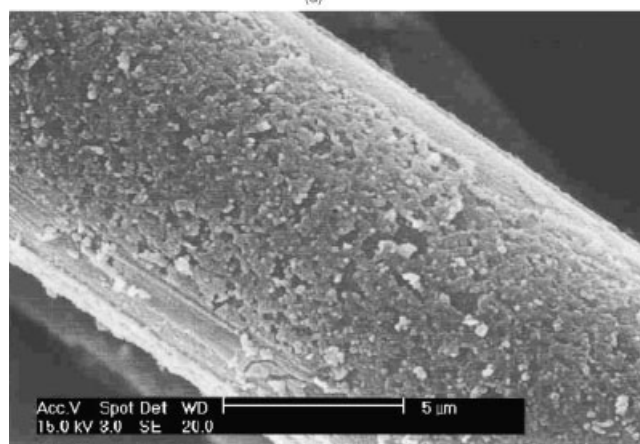
**TABLE I**  
Effective Diffusion Coefficients of Polymer and Composite Specimens

Fiber volume fraction (%)	Maximum moisture content (%)	Diffusion coefficient, $D$ ( $10^{-8}$ cm <sup>2</sup> /s)	
		Shorter times	Longer times
0	0.38	11.4	12.6
10	1.81	14.2	15.5
20	2.42	15.9	17.9
0 <sup>a</sup>	0.62	20.4	–

<sup>a</sup>Aitchison et al.<sup>15</sup>



(a)



(b)

**Figure 2** Sized phosphate glass fibers: as prepared (a) and after 6 weeks (b) of water immersion.

the mass loss data in Figure 1, which indicate that the process is aggressive for the first 96 h of immersion. The subsequent mass loss is stabilized beyond 200 h, which may indicate saturation. SEM images help to reveal the interaction of PG fiber bundles and water. There are evident pits and formation of precipitates on the fiber surface after 6 weeks [Fig. 2(b)].

The hydrolytic degradation of PG fiber composites relies upon the interaction of water molecules with the molecular chains of both the polymer and the phosphate glass. Here, different rates of hydrolysis will lead to the scission of macromolecular chains, particularly in the PG fibers. The degradation period can therefore be summarized in three phases, which might be more or less coincident depending upon the solubility of the individual phases:

- Moisture ingress via diffusion, manifested by mass gain.
- Chemical interaction between water and macromolecular chains of degradable polymers.
- Leaching of ions after scission of macromolecules, manifested by mass loss.

Figure 1 demonstrates clearly the transition from the initial, diffusion-dominated behavior to a leaching effect, the changeover occurring at  $\sim 234$  h of exposure (for  $V_f = 20\%$ ). It is interesting to consider that the point at which the net mass change becomes negative is significantly different for the two different fiber ratios. Although it follows that the initial moisture ingress is dominated by voids, rather than the saturation of the polymer alone, the void fraction, rather than the fiber fraction, might be the main determinant of this event.

Degradation data for particulate PG-PCL composite given by Prabhakar et al.<sup>10</sup> are more rapid than the results given in Figure 1 and may be attributable to different glass formulations  $((\text{Na}_2\text{O})_{0.55-x}(\text{CaO})_x(\text{P}_2\text{O}_5)_{0.45}$  in Prabhakar et al.) and to the form of the reinforcements, since both surface area and residual stress levels will influence dissolution rates. Prabhakar et al.<sup>10</sup> also point out internal voids and microcracks as a means of accelerating dissolution in the aqueous environment. Note also that sizing with 3-aminopropyl triethoxy silane coating the fiber surface may also protect the fibers from rapid hydrolysis, in addition to its main duty as an adhesion promoter. This contribution of the sizing agent in affecting the dissolution rate of phosphate glass fibers has also been emphasized by Rinehart et al.<sup>7</sup>

SEM examination of degrading specimens helps to elicit further the effects of the wet environment. After degradation in water for 6 weeks, leaching of the glass was almost complete with very significant internal porosity in the remaining polymer visible in Figure 3(b).

### Moisture uptake

Fick's second law is commonly used to approximate the moisture uptake for homogenous and isotropic materials. Here we examine its use to approximate the behavior of this heterogeneous, orthotropic material, noting the representative microstructure and distribution of phosphate glass fibers in Figure 3(a).

The analytical model is based on the following assumptions:

- The problem is dominated by transverse diffusion of the fluid and in-plane diffusion is negligible.
- The specimen is exposed to a uniform boundary conditions (i.e., the saturation at all surfaces remains uniform, as do all properties of the fluid).
- The specimen has a uniform initial saturation.
- The only mass transfer occurs due to diffusion in or out of the sample (i.e., the rate of hydrolytic degradation is small compared to the rate of diffusion).
- The specimen has an effective diffusion coefficient as described later.

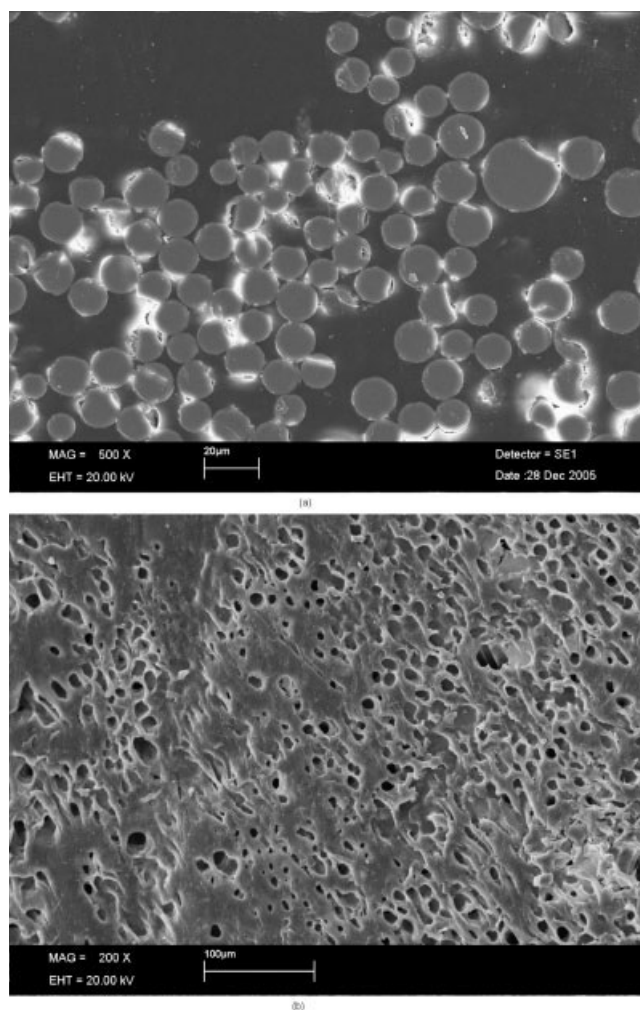


**Figure 3** Phosphate glass fiber-PCL transverse section at  $V_f = 10\%$ . Ground section, as molded. Following 6 weeks of exposure to double-distilled water at  $37^\circ\text{C}$ .

According to the assumptions listed earlier, the water concentration in the  $z$ -direction (through the thickness of the sample) can be generated for a composite lamina by a one-dimensional diffusion equation based upon Fick's second law.<sup>16</sup>

$$\frac{\partial c(z,t)}{\partial t} = D \frac{\partial^2 c(z,t)}{\partial z^2} \quad (0 \leq z \leq h, \quad t > 0)$$

$$c = c_0 \quad (0 < z < h, \quad t \leq 0)$$

$$c = c_{\text{max}} \quad (z = 0, \quad z = h, \quad t > 0)$$
(2)

where  $c$  is moisture concentration or saturation,  $D$  is diffusion coefficient of the material in the direction normal to the surface,  $h$  is thickness of specimen,  $t$  is time,  $z$  is distance measured from the bottom surface, and subscripts "0" and "max" represent initial and maximum moisture absorbed states, respectively.

Maximum moisture concentration is used here rather than assuming that the process runs to a fully saturated state. This is because (for the case of rela-

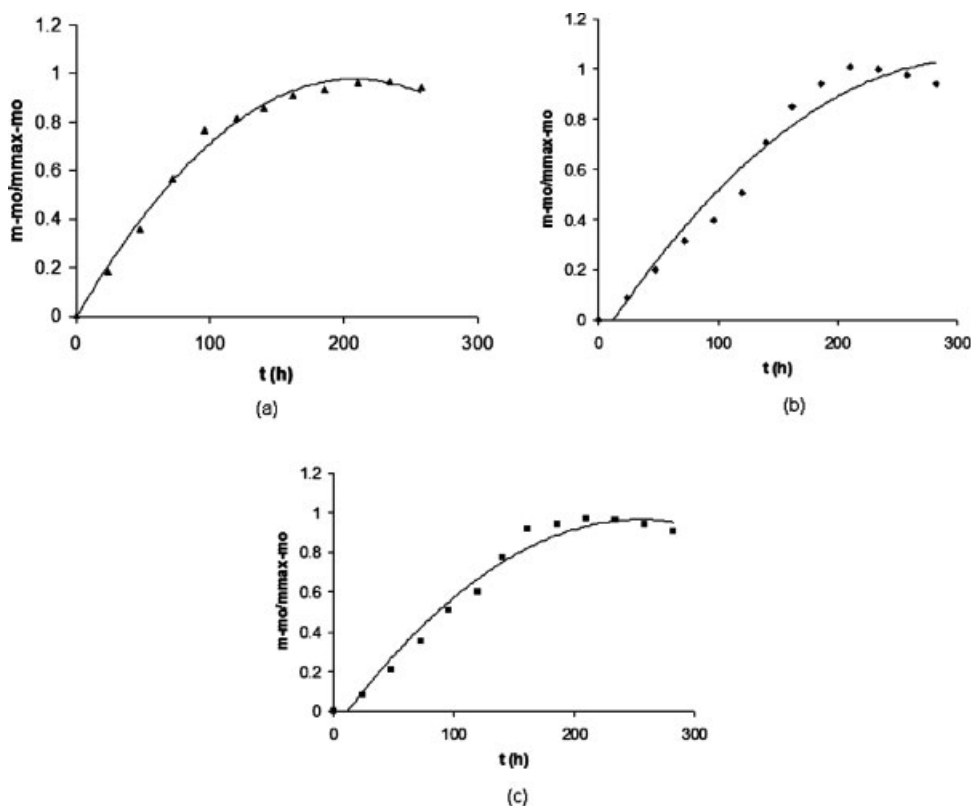


**Figure 4** Normalized weight fraction of the fiber-reinforced composites for  $V_f$  0% (unreinforced PCL polymer) (a),  $V_f$  10% (b), and  $V_f$  20% (c) composites.

tively soluble fibers) the moisture content will promote dissolution and leaching of glass and the usual equilibrium value may not be attained (as demonstrated for the fiber loaded specimens in Fig. 3).

The moisture concentration depends on  $z$  and  $t$ , and is therefore defined as;  $c = \lim_{\Delta V \rightarrow 0} \frac{\text{mass of water absorbed in volume } \Delta V}{\text{mass of dry material of volume } \Delta V}$ . Hence, the following solution<sup>17</sup> is deduced from eq. (2).

$$\frac{c - c_0}{c_{\max} - c_0} = 1 - \frac{4}{\pi} \sum_{n=0}^{\infty} \frac{1}{(2n+1)^2} \sin \frac{(2n+1)\pi z}{h} \times \exp \left[ -\pi^2 (2n+1)^2 \frac{Dt}{h^2} \right] \quad (3)$$

if this equation is integrated over the plate thickness

$$m = \int_0^h c dx \quad (4)$$

and the result of this integration is

$$G \equiv \frac{m - m_0}{m_{\max} - m_0} = 1 - \frac{8}{\pi^2} \sum_{n=1}^{\infty} \frac{1}{(2n+1)^2} \exp \left[ -\pi^2 (2n+1)^2 \frac{D_L t}{h^2} \right] \quad (5)$$

where  $G$  is a time-dependent parameter (relative moisture regain),  $m_{\max}$  is the mass of the sample at maximum moisture concentration and  $m_0$  is the dry weight when  $t = 0$ .

Experimental values fitted to eq. (5) yield the effective diffusion coefficient ( $D_L$ ) for longer times, and the moisture uptake curves are presented in Figure 4 at varying fiber loadings. Note that the unreinforced polymer data provide a better fit to eq. (5) than do the fiber-reinforced samples, and this may be because, as speculated earlier, this set were thought to contain significantly greater voidage than the cast polymer alone.

#### Diffusion coefficient

Shen and Springer<sup>18</sup> discussed an analytical model of moisture absorption for one-dimensional problem. The relations were based on Fick's law. The effective diffusion constant for short times ( $D_S$ ) was calculated with the simple equation given as follows.<sup>18</sup>

$$D_S = \frac{\pi}{16} \left( \frac{h}{R_{\max}} \right)^2 \left( \frac{dR}{d\sqrt{t}} \right)^2 \quad (6)$$

The initial gradient for all sample groups were determined from lines of best fit given in Figure 5. The

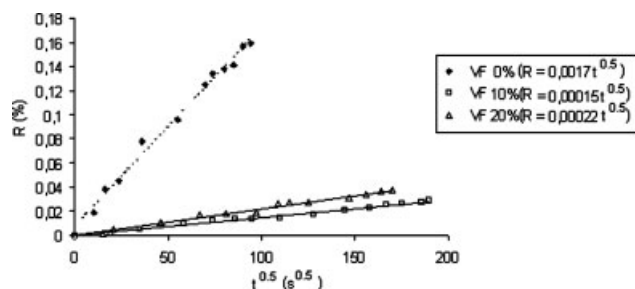


**Figure 5** Percentage moisture regain versus the square root of immersion time.

diffusivity constant for the composites was calculated using eq. (6).

Table I summarizes the values calculated for the effective diffusion coefficients at shorter and longer times. It should be noted that the calculated coefficients depend strongly on the microstructure of the specimen, which changes between dry and maximum concentration because of fiber leaching. The diffusivity constant for pure PCL composite is almost half that reported by Aitchison et al.<sup>15</sup>

## CONCLUSIONS

Moisture regain of phosphate glass fiber-PCL matrix composites was studied in distilled water at 37°C for different volume ratios of fiber. The maximum moisture content increased with the fiber loading. Previous work suggests that solubility of PCL is significantly lower than phosphate glass fibers, and this is confirmed by the flat signature of the PCL samples. The fiber-containing specimens leached significant quantities of glass over the 6-week experiment, and this contributed to an evolving microstructure and porosity during the initial, diffusion-dominated period. Fitting a one-dimensional form of Fick's second law permits the diffusion to be approximated and the overall diffusion coefficient increased with vol-

ume fraction of fiber, which may be due to internal voidage in the specimens.

Levent Onal appreciates the support and understanding of Professor Christopher D. Rudd and his research team during the research period. The help of Ruhul Amin Khan and Yang Jing during fiber spinning and preparation is highly appreciated.

## References

- Ramakrishna, S.; Mayer, J.; Wintermantel, E.; Leong, K. W. *Comp Sci Technol* 2001, 61, 1189.
- Thomas, P.; Maier, S.; Summer, B. *Material-wissenschaft und Werkstofftech* 2004, 35, 997.
- Jones, J. R.; Hench, L. L. *Mater Sci Technol* 2001, 17, 891.
- Hutmacher, D. W.; Schantz, T.; Zein, I.; Teoh, S. H.; Tan, K. C. *J Biomed Mater Res* 2001, 55, 203.
- Maas, C. S.; Mervin, G. E.; Wilson, J.; Frey, M. D.; Maves, M. D. *Arch Otolaryngol Head Neck Surg* 1990, 116, 551.
- Kulkarni, R. K.; Moore, E. G.; Hegyeli, A. F.; Leonardo, F. J. *Biomed Mater Res* 1971, 5, 169.
- Rinehart, J. D.; Taylor, T. D.; Tian, Y.; Latour, R. A. *J Biomed Mater Res* 1999, 48, 833.
- Kweon, H. Y.; Yoo, M. K.; Park, K.; Kim, T. H.; Lee, H. C.; Lee, H.; Oh, J.; Akaike, T.; Cho, C. S. *Biomaterials* 2003, 24, 801.
- Middleton, J. C.; Tipton, A. J. *Biomaterials* 2000, 21, 2335.
- Prabhakar, R. L.; Brocchini, S.; Knowles, J. C. *Biomaterials* 2005, 26, 2209.
- Corden, T. J.; Jones, I. A.; Rudd, C. D.; Christian, P.; Downes, S.; McDougal, K. E. *Biomaterials* 2000, 21, 713.
- Gough, J. E.; Christian, P.; Scotchford, C. A.; Rudd, C. D.; Jones, I. A. *J Biomed Mater Res* 2002, 59, 481.
- Corden, T. J.; Jones, I. A.; Rudd, C. D.; Christian, P.; Downes, S. *Compos A* 1999, 30, 737.
- Jiang, G.; Jones, I. A.; Rudd, C. D.; Walker, G. S. *Polymer* 2003, 44, 1809.
- Aitchison, G. A.; Walker, G. S.; Jones, I. A.; Rudd, C. D. *J Appl Polym Sci*, submitted.
- Crank, J. *The Mathematics of Diffusion*; Oxford University Press, New York, 1970; Chapters IV, V, and VI.
- Jost, M. *Diffusion in Solids, Liquids and Gases*; Academic Press, New York, 1960.
- Shen, C-H.; Springer, G.S. *Environmental Effects on Composite Materials*; Springer, G. S., Ed.; Technomic Publishing, Lancaster, 1981; pp 16–33.